Deterministic protocol for mapping a qubit to coherent state superpositions in a cavity

Zaki Leghtas,[1,2,*] Gerhard Kirchmair,[2] Brian Vlastakis,[2] Michel H. Devoret,[2] Robert J. Schoelkopf,[2] and Mazyar Mirrahimi[1,2]
[1]*INRIA Paris-Rocquencourt, Domaine de Voluceau, Boîte Postale 105, 78153 Le Chesnay Cedex, France*
[2]*Department of Physics and Applied Physics, Yale University, New Haven, Connecticut 06520, USA*
(Received 31 May 2012; published 15 April 2013)

We propose and analyze a quantum gate that transfers an arbitrary state of a qubit into a superposition of two quasiorthogonal coherent states of a cavity mode (qcMAP), with opposite phases. This qcMAP gate is based on conditional qubit and cavity operations exploiting the energy-level dispersive shifts in the regime where they are much stronger than the cavity and qubit linewidths. The generation of multicomponent superpositions of quasiorthogonal coherent states, nonlocal entangled states of two resonators, and multiqubit Greenberger-Horne-Zeilinger states can be efficiently achieved by this gate.

DOI: 10.1103/PhysRevA.87.042315 PACS number(s): 03.67.Lx, 42.50.Dv, 42.50.Pq, 85.25.−j

I. INTRODUCTION

In the field of quantum Josephson circuits, microwave resonators are extremely useful for performing readouts, coupling multiple qubits, and protecting against decoherence [1–3]. In addition, using an oscillator as a memory to store a qubit state has been explored both theoretically and experimentally (see, e.g., Refs. [4–6]). The recent improvement in coherence times of microwave resonators with respect to superconducting qubits [7,8] makes it particularly interesting to use a cavity as a quantum memory in this context.

In this article we propose and analyze a gate between a qubit and a cavity (qcMAP) which maps the qubit state onto a superposition of two quasiorthogonal coherent states with opposite phases. This gate provides access to the large Hilbert space of the cavity, so that one can encode the information of a multiqubit system on a single-cavity mode and decode it back on the qubits. In particular, this gate can be employed to efficiently prepare any superposition of quasiorthogonal coherent states (SQOCS) [9,10]. Furthermore, we show that this scheme can be easily adapted to prepare entangled states of two resonators [11], which would maximally violate Bell's inequality.

This qcMAP gate, combined with the previously demonstrated capabilities of circuit QED, yields a very powerful quantum manipulation toolbox and opens a new paradigm for working with the coherent states of an oscillator. The new approach we introduce in this paper, in comparison with previous ones, is characterized by three advantages. First, we require only a minimal setup with fixed qubit-cavity couplings and frequencies, maximizing coherence. Second, we can directly prepare superpositions of coherent states without the lengthy procedure of synthesizing them from Fock states one by one [12]. Hence, the time to prepare a SQOCS using the qcMAP gate does not increase with the amplitudes of the coherent components, but scales only linearly with the number of coherent components. Large SQOCS could therefore be generated with high fidelities to explore the decoherence of highly nonclassical states [13,14]. Finally, our scheme is fully deterministic and reversible, allowing it to serve as a basis for more complicated tasks such as quantum error correction [15].

*Corresponding author: zaki.leghtas@yale.edu

II. THE qcMAP GATE

We place ourselves in the strong dispersive regime, where both the qubit and resonator transition frequencies split into well-resolved spectral lines indexed by the number of excitations in the qubit and the resonator [16]. The resonator frequency ω_r splits into two well-resolved lines, ω_r^g and ω_r^e, corresponding to the cavity's frequency when the qubit is in the ground ($|g\rangle$) or the excited ($|e\rangle$) state. Through the same mechanism, the qubit frequency ω_q splits into $\{\omega_q^n\}_{n=0,1,2,\ldots}$ corresponding to the qubit frequency when the cavity is in the photon number state $|n\rangle$. Recent experiments have shown dispersive shifts that are about three orders of magnitude larger than the qubit and cavity linewidths [3].

The qcMAP gate relies on two operations which we detail in the following: the conditional cavity displacement, which we denote by D_α^g, and the conditional qubit rotation, which we denote by X_θ^0 [see Fig. 1(a)]. An *un*conditional displacement D_α is obtained by applying a very short pulse, which displaces a coherent state by α regardless of the qubit state. A conditional displacement D_α^g can be realized in the strong dispersive limit: with a selective pulse of duration $T \gtrsim 1/\chi_{\rm qr}$ ($\chi_{\rm qr}$ being the dispersive shift of the cavity frequency when the qubit is excited), we may displace the cavity by a complex amplitude α only if the qubit is in the ground state. For a coherent state $|\beta\rangle$, we have $D_\alpha^g|e,\beta\rangle = |e,\beta\rangle$ and $D_\alpha^g|g,\beta\rangle = e^{(\alpha\beta^\dagger-\alpha^\dagger\beta)/2}|g,\beta+\alpha\rangle$. Such a conditional displacement was first proposed in [17] as part of a nondeterministic scheme to prepare a two-component superposition of coherent states. In [18], this nondeterministic preparation followed by high-fidelity measurements and real-time feedback was used to perform various quantum gates. More recently, the conditional displacement was combined with unconditional qubit rotations to render the preparation deterministic [11]. The unconditional qubit rotations would necessitate decoupling the qubit from the cavity and hence require real-time frequency tuning. For the deterministic qcMAP gate with no real-time qubit frequency tuning, we combine this displacement with a conditional qubit rotation, X_π^0. The conditional rotations X_θ^0 are simply achieved by applying a selective pulse at ω_q^0, performing a rotation of angle θ of the qubit state conditioned on the cavity being in its vacuum state. Such selective qubit rotations have been experimentally demonstrated in [19].

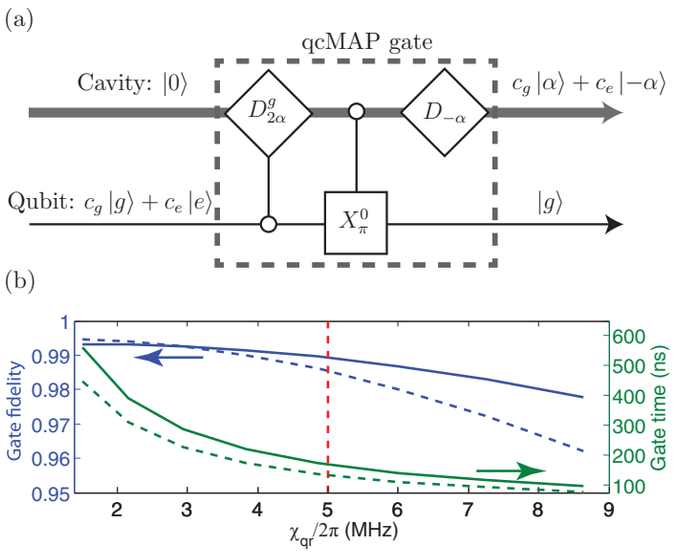

FIG. 1. (Color online) (a) The qcMAP gate comprises a conditional displacement of the cavity mode $D^g_{2\alpha}$ and a conditional rotation of the qubit X^0_π, mapping the qubit state to a superposition of two coherent states with opposite phases in the cavity. (b) Fidelity (blue) and gate time (green) of the qcMAP gate as a function of the dispersive coupling χ_{qr}, for two values, 3.5 (solid line) and 7 (dashed line), of $\bar{n} = |\alpha|^2$. Increasing χ_{qr} decreases the gate time, however it also increases the cavity self-Kerr χ_{rr}, which reduces the fidelity. This effect is more important for large coherent states, which explains the more important fidelity drop for $\bar{n} = 7$ photons. For $\bar{n} = 3.5$ photons, fidelities larger than 99% are obtained for χ_{qr} smaller than 5 MHz, with a gate time of ≈170 ns, much shorter than achievable coherence times.

In order to map the state of the qubit to the cavity mode, we construct the qcMAP gate as follows. Starting from a qubit in $c_g|g\rangle + c_e|e\rangle$ and a cavity in $|0\rangle$, the first conditional displacement $D^g_{2\alpha}$ entangles the qubit and the cavity, creating the state $c_g|g,2\alpha\rangle + c_e|e,0\rangle$. We choose $2|\alpha|$ to be large enough so that the nonorthogonality of the two coherent states $|\langle 2\alpha|0\rangle|^2 = e^{-4|\alpha|^2}$ is negligible (of order 10^{-6} for $\bar{n} = |\alpha|^2 = 3.5$). The conditional π pulse X^0_π can then disentangle the qubit from the cavity leaving the qubit in $|g\rangle$ and the cavity in $c_g|2\alpha\rangle + c_e|0\rangle$. Finally, the unconditional displacement $D_{-\alpha}$ centers the superposition at the origin.

The qcMAP gate is well adapted to quantum-information processing with a transmon qubit [20] coupled to a microwave resonator. The Hamiltonian is well approximated by [21]

$$\frac{\mathbf{H}}{\hbar} = \omega_r \mathbf{a}^\dagger\mathbf{a} + \omega_q \mathbf{b}^\dagger\mathbf{b} - \frac{\chi_{rr}}{2}(\mathbf{a}^\dagger\mathbf{a})^2 - \frac{\chi_{qq}}{2}(\mathbf{b}^\dagger\mathbf{b})^2 - \chi_{qr}\mathbf{a}^\dagger\mathbf{a}\mathbf{b}^\dagger\mathbf{b}.$$

Here $\mathbf{a}$ and $\mathbf{b}$ are, respectively, the dressed mode operators of the resonator and the qubit ($|g\rangle$ and $|e\rangle$ are the first two eigenstates of $\mathbf{b}^\dagger\mathbf{b}$), ω_r and ω_q are their frequencies, χ_{qr} is the dispersive qubit-resonator coupling, and χ_{qq} and χ_{rr} the anharmonicities. Indeed, due to the coupling to a nonlinear medium (the qubit), the cavity also inherits a Kerr effect that leads to the anharmonicity $\chi_{rr} = \chi_{qr}^2/4\chi_{qq}$ [21]. This nonlinearity can distort coherent states and sets a limit on the fidelity of the gate.

While the unconditional cavity displacement D_α can be performed rapidly using a short pulse, the conditional cavity displacements D^g_α and qubit rotations X^0_θ necessitate long pulses allowing one to selectively address the corresponding spectral line. In the qcMAP gate, X^0_π transforms $|e,0\rangle$ to $|g,0\rangle$ while leaving $|g,2\alpha\rangle$ unchanged. To this end, we apply a pulse with the carrier frequency ω^0_q and shape it such that it does not overlap with the spectral lines $\omega^n_q (= \omega^0_q - n\chi_{qr})$ corresponding to the qubit frequencies when the cavity is in $|2\alpha\rangle$. Indeed, ideally a conditional qubit rotation should act as the identity whenever the cavity is in any photon number state other than the vacuum. However, here we only need it to leave the qubit state unchanged when the cavity is in the state $|2\alpha\rangle$. Defining $\bar{n} = \langle\alpha|\mathbf{a}^\dagger\mathbf{a}|\alpha\rangle = |\alpha|^2$, the pulse length needs to be longer than a certain multiple of $1/4\bar{n}\chi_{qr}$. Here we take a Gaussian pulse of standard deviation $\sigma_t = 5/4\bar{n}\chi_{qr}$ and total length $6\sigma_t$ resulting in a π-pulse time of $15/2\bar{n}\chi_{qr}$ (≈70 ns for $\bar{n} = 3.5$ and $\chi_{qr}/2\pi = 5$ MHz) for 99% fidelity. For the D^g_α operation, using a Gaussian pulse to selectively address ω^g_r without driving $\omega^e_r = \omega^g_r - \chi_{qr}$ (the spectral lines are separated by χ_{qr} and not $4\bar{n}\chi_{qr}$) would require a relatively long time of $\approx 30/\chi_{qr}$. However, as detailed in Appendix A, D^g_α can be performed using two unconditional displacements and a waiting time between them [11]; the whole operation time is significantly reduced to π/χ_{qr} (≈100 ns). The total gate time is $T_{\text{Gate}} \approx \frac{15+2\bar{n}\pi}{2\bar{n}\chi_{qr}}$ ($T_{\text{Gate}} \approx 170$ ns).

There is a compromise between decreasing the gate time with larger coupling strengths and increasing the undesirable effect of the cavity self-Kerr. The Kerr effect leads to a phase collapse of a coherent state with the mean photon number $\bar{n}$ on a time scale of $T_{\text{collapse}} = \frac{\pi}{2\sqrt{\bar{n}}\chi_{rr}}$ ([22], Sec. 7.2) (see also [23]). This phase collapse can be considered as an extra dephasing of the cavity and reduces the gate fidelity.

In Fig. 1(b), we compute the fidelity and time of the qcMAP gate in the presence of the cavity self-Kerr but without any decoherence. We take $\chi_{qq}/2\pi = 300$ MHz and vary χ_{qr}. The fidelity F of the gate $\mathcal{U}$ is defined as $F = \min_{c_g,c_e} |(c^\dagger_g\langle g,\alpha| + c^\dagger_e\langle g,-\alpha|)\mathcal{U}(c_g|g,0\rangle + c_e|e,0\rangle)|^2$. The gate fidelity and the gate time decrease with increasing χ_{qr}. The decrease in fidelity is slightly worse for higher $\bar{n}$ since the coherent state becomes more exposed to the cavity's nonlinearity. The maximum fidelity of ≈99.5% is set by the fidelity of the conditional π pulse which can be arbitrarily improved using longer pulses (at the expense of longer gate times). In the presence of decoherence, one should increase the coupling strength (and therefore decrease the gate time) up to values that make the phase collapse due to the cavity self-Kerr comparable to other dephasing times.

III. APPLICATIONS OF THE qcMAP GATE

A. Preparation of arbitrary superpositions of quasiorthogonal coherent states

One can tailor any SQOCS by applying a sequence of qcMAP gates (see [10] for another method based on the dynamical quantum Zeno effect, and see [24] for a nondeterministic scheme). The protocols to generate two-, three-, and 4-component SQOCS are given in Figs. 2(a)–2(c). The master equation simulation of these preparation protocols leads to the

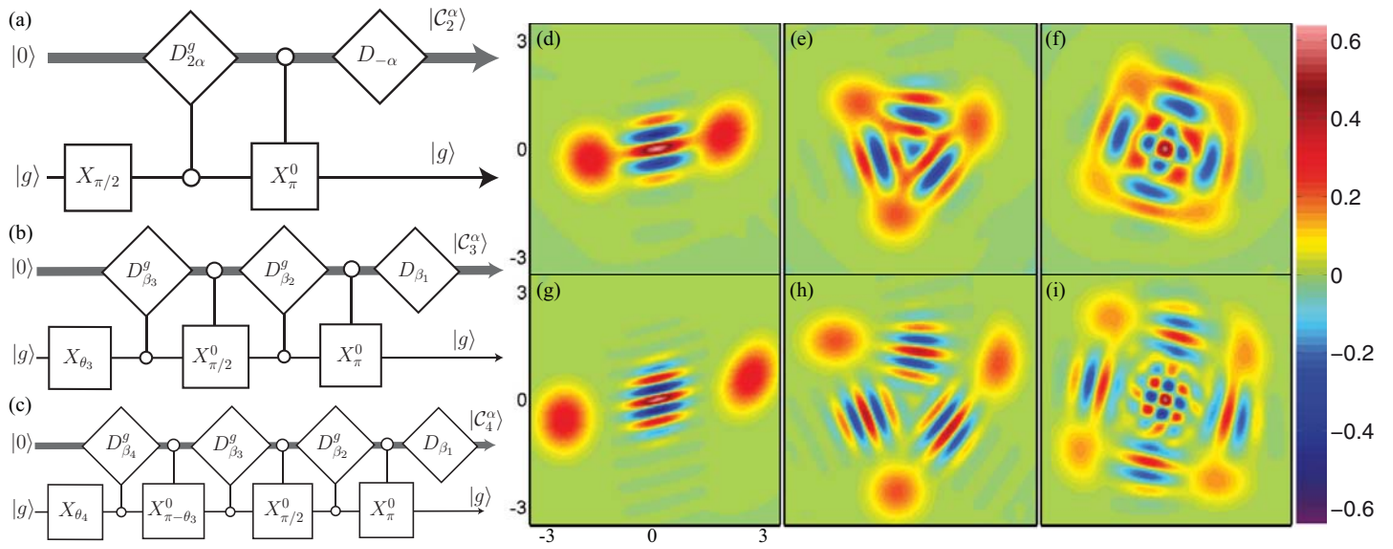

FIG. 2. (Color) (a–c) Operations to prepare a two-component (a), three-component (b), and four-component (c) SQOCS. $|\mathcal{C}_n^\alpha\rangle$ denotes a superposition of coherent states $|\alpha_1\rangle + \cdots + |\alpha_n\rangle$. In panels (b) and (c), $\beta_1 = \alpha_1$, $\beta_2 = \alpha_2 - \alpha_1$, $\beta_3 = \alpha_3 - \alpha_2$, and $\theta_3 = 2\arccos(1/\sqrt{3})$. In addition, in panel (c), $\beta_4 = \alpha_4 - \alpha_3$ and $\theta_4 = 2\arccos(1/2)$. (d–i) Wigner functions of the prepared states in the presence of decoherence and the cavity self-Kerr. The upper figures correspond to $\bar{n} = 3.5$ photons in each coherent component and the lower ones correspond to 7 photons. We define the fidelity of the prepared state ρ_{prep} to the target $|C_n^\alpha\rangle$ as $F_{\text{prep}}(|C_n^\alpha\rangle) = \langle C_n^\alpha|\rho_{\text{prep}}|C_n^\alpha\rangle$. We get $F_{\text{prep}}(|\mathcal{C}_2^\alpha\rangle) = 97.8\%$ (respectively, 97.2%) for $\bar{n} = 3.5$ (respectively, $\bar{n} = 7$) for a preparation time $T_{\text{prep}} = 170$ ns (respectively, 135 ns). Similarly, $F_{\text{prep}}(|\mathcal{C}_3^\alpha\rangle) = 96.2\%$ (respectively, 95.7%) and $T_{\text{prep}}(|\mathcal{C}_3^\alpha\rangle) = 320$ ns (respectively, 225 ns); $F_{\text{prep}}(|\mathcal{C}_4^\alpha\rangle) = 91.9\%$ (respectively, 91.5%) and $T_{\text{prep}}(|\mathcal{C}_3^\alpha\rangle) = 460$ ns (respectively, 355 ns). Note the insensitivity of the preparation fidelity to the size of the coherent components. Due to the cavity self-Kerr, the components that are created earlier are deformed more than those created later.

Wigner functions shown in Figs. 2(d)–2(i). The corresponding parameters are $\chi_{\text{qr}}/2\pi = 5$ MHz, $\chi_{qq}/2\pi = 300$ MHz, and $\chi_{rr}/2\pi = 20$ kHz. The qubit relaxation and dephasing times are $T_1 = T_2 = 20$ μs, and the cavity decay time is $T_{\text{cav}} = 100$ μs. Recent experiments with transmon qubits coupled to three-dimensional resonators [3,25] indicate that such parameters are realistic. More details on the preparation scheme can be found in Appendix A. In particular, one notes the insensitivity of the fidelity to the size of the coherent components. The ability to prepare multicomponent SQOCS also implies that the qcMAP gate can be used to store *multi*qubit states in the resonator.

B. Entanglement of two spatially separated cavity modes

The qcMAP gate can also be used on a qubit coupled to two spatially separated cavities [26] to prepare *nonlocal* mesoscopic superposition states of the form $|-\alpha,-\alpha\rangle + |\alpha,\alpha\rangle$. Such highly nonclassical states achieve a maximum violation of Bell's inequality as soon as $|\alpha|^2 \approx 2$ [[22], Sec. 7.6]. The preparation scheme is sketched in Fig. 3. As in the single-mode case, the sequence duration is set by the length of the selective operations. The two conditional displacements are performed simultaneously and their time is given by $\max(\pi/\chi_{qr_1}, \pi/\chi_{qr_2})$ (χ_{qr_1} and χ_{qr_2} being the dispersive coupling between the qubit and cavity modes). The conditional π pulse is performed in a time of order $15/2\bar{n}(\chi_{qr_1} + \chi_{qr_2})$. Therefore, the preparation time for a nonlocal superposition is even shorter than that for the single-mode case. However, in addition to the cavity self-Kerr effects $\chi_{r_1r_1}$ and $\chi_{r_2r_2}$, we also have a cross-Kerr term, $\chi_{r_1r_2}\mathbf{a}_1^\dagger\mathbf{a}_1\mathbf{a}_2^\dagger\mathbf{a}_2$, between the two modes ($\chi_{r_1r_2}$ is given by $2\sqrt{\chi_{r_1r_1}\chi_{r_2r_2}}$ [21]).

We simulate this scheme taking $\chi_{qr_1}/2\pi = 5$ MHz, $\chi_{qr_2}/2\pi = 4$ MHz, $\chi_{r_1r_2}/2\pi = 20$ kHz, $\chi_{r_1r_1}/2\pi = 20$ kHz, $\chi_{r_2r_2}/2\pi = 13$ kHz, and $\chi_{qq}/2\pi = 300$ MHz and taking coherence times of $T_1 = T_2 = 20$ μs for the qubit and $T_{\text{cav}} = 100$ μs for the two cavities. The entangled state $|\alpha,\alpha\rangle + |-\alpha,-\alpha\rangle$ with $|\alpha|^2 = 1.5$ is prepared with a fidelity of $\approx$96% in 190 ns. By calculating the two-mode Wigner function at four points, as explained in [27–29], we retrieved a Bell signal of 2.5, largely violating Bell's inequality (maximum possible Bell signal is $2\sqrt{2}$).

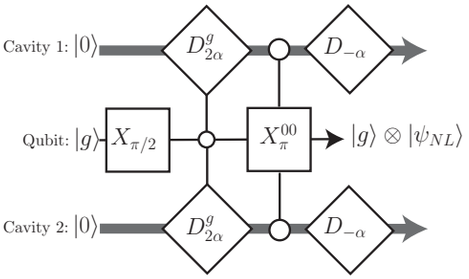

FIG. 3. Protocol for preparing a nonlocal entangled state between two cavities that are dispersively coupled to a single qubit. Two simultaneous conditional displacements lead to a tripartite entanglement, preparing the state $|g,2\alpha,2\alpha\rangle + |e,0,0\rangle$. A π pulse on the qubit, conditioned on both cavities being in vacuum, will then disentangle the qubit from the cavities leaving them in an entangled state $|\psi_{\text{NL}}\rangle = (|-\alpha,-\alpha\rangle + |\alpha,\alpha\rangle)/N$, where N is a normalization constant. We obtain a fidelity of $\approx$96% in 190 ns, leading to a Bell signal of 2.5.

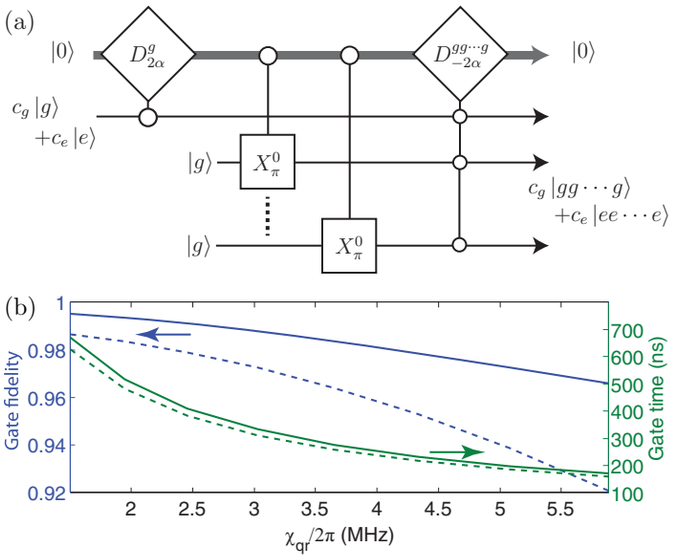

FIG. 4. (Color online) (a) The qcMAP gate can be used to map a single-qubit state $c_g|g\rangle + c_e|e\rangle$ to a GHZ-type state $|\mathrm{GHZ}\rangle = c_g|gg\cdots g\rangle + c_e|ee\cdots e\rangle$ for an arbitrary number of qubits. The conditional rotations of qubits can be done in parallel and therefore the total preparation time does not increase with the number of qubits n_q (it actually slightly decreases with n_q since the conditional displacement $D^{gg\cdots g}_{-2\alpha}$ can be performed faster). (b) Gate fidelity (blue) and time (green) as a function of the dispersive coupling strength for three (solid lines) and five qubits (dashed lines); we take the same dispersive shifts χ_{qr} for all qubits (not a necessary assumption) and $|\alpha|^2 = 3.5$. Like in Fig. 1, the simulation does not include decoherence but takes into account the cavity self-Kerr. For larger n_q, the cavity self-Kerr increases which leads to a drop in gate fidelity, particularly for high dispersive coupling strengths. We obtain fidelities in excess of 99% (respectively, 98%) for $n_q = 3$ (respectively, $n_q = 5$) with a gate time of 400 ns.

C. Multiqubit gates

We have shown that the qcMAP gate generates highly nonclassical cavity field states, making it a promising tool to store multiqubit states in the cavity [4,30,31]. An extension of the qcMAP gate uses the cavity as a bus to perform multiqubit gates. As shown in Fig. 4(a), starting from state $c_g\,|g\rangle + c_e\,|e\rangle$ for one qubit, we use the qcMAP gate to map this state to a multiqubit entangled state $c_g\,|gg\cdots g\rangle + c_e\,|ee\cdots e\rangle$. A first conditional displacement $D^{g}_{2\alpha}$ prepares $c_g\,|2\alpha, gg\cdots g\rangle + c_e\,|0, eg\cdots g\rangle$. The time for this operation is $\approx\pi/\chi_1$. Applying, in parallel, a conditional π pulse X^0_π on $n_q - 1$ qubits, we prepare an (n_q+1)-body entangled state $c_g\,|2\alpha, gg\cdots g\rangle + c_e\,|0, ee\cdots e\rangle$. The time for this operation is fixed by the minimum dispersive coupling strength. Next, we perform a conditional displacement $D^{gg\cdots g}_{-2\alpha}$ disentangling the cavity from the qubits which are left in $c_g\,|gg\cdots g\rangle + c_e\,|ee\cdots e\rangle$, while the cavity is in vacuum. This conditional displacement can be performed in a very short time, $\approx\pi/(\chi_1 + \cdots + \chi_{n_q})$, which decreases with the number of qubits. Such an operation can be compared to the joint readout of qubits in the strong dispersive regime [32,33] where, by driving the cavity at a frequency corresponding to a particular joint state of qubits, one can measure its population with a high fidelity.

In Fig. 4(b), we plot the gate time and fidelity as a function of the dispersive coupling χ_{qr}. A limiting effect on the fidelity is the cavity self-Kerr which increases additively with the number of qubits. Despite this effect, for $\chi_{\mathrm{qr}}/2\pi = 3$MHz, we prepare a five-qubit Greenberger-Horne-Zeilinger (GHZ) state with an $\approx$97.5% fidelity in 300 ns. Furthermore, this gate can be performed between any subset of qubits coupled to the bus and does not require any qubit tunability or employment of higher excited states.

Such an application of a cavity mode as a bus to perform multiqubit gates can be compared to the scheme proposed in [34] and some further work following this paper which is well summarized in [35]. In these works, conditional displacements are concatenated to obtain such gates in near-deterministic ways. However, similarly to [11], they require the ability to couple and decouple qubits from the cavity at will.

IV. CONCLUSION

In conclusion, we have introduced the qcMAP gate which maps a qubit state to a superposition of two coherent states in a cavity. The qcMAP gate is then used to prepare two-, three-, and four-component SQOCS, as well as a nonlocal mesoscopic field state superposition in two cavity modes. Using this gate, the resonator could be used as a quantum "disk drive" to store multiqubit states in a multicomponent SQOCS. A SQOCS of maximum photon number $\bar{n}$, for which the maximum nonorthogonality of two coherent components is e^{-4m}, could store a register of $\approx \log_2(\bar{n}/m)$ qubits. The effective decay rate of such a state would be $\bar{n}\kappa$ where κ is the decay rate of one photon. Using the qcMAP gate, the cavity can also be used as a bus to perform a multiqubit gate, preparing, in particular, GHZ states. Finally, any multiqubit gate can be performed by concatenating such qcMAP gates.

ACKNOWLEDGMENTS

This work was partially supported by the French "Agence Nationale de la Recherche" under Project EPOQ2 (No. ANR-09-JCJC-0070) and the Army Research Office (ARO) under Project No. ARO-W911NF-09-1-0514, and the NSF DMR-1004406. Z.L. acknowledges support from the Fondation Sciences Mathématiques de Paris.

APPENDIX A: SEQUENCE OF OPERATIONS WHICH PREPARES THE TWO-, THREE-, AND FOUR-COMPONENT SQOCS

In this section, we describe in detail the D^g_α operation and provide the full sequence of steps that prepares the two-, three-, and four-component superposition of quasiorthogonal coherent states with performances announced in this article.

While the conditional qubit rotation X^0_θ is performed through long enough pulses ensuring a selective addressing of spectral lines (see main text), the conditional cavity displacement D^g_α is composed of two short unconditional displacements separated by a waiting time. This reduces the D^g_α operation time from $\approx 30/\chi_{\mathrm{qr}}$ to $\approx\pi/\chi_{\mathrm{qr}}$. We consider the rotating frame of the Hamiltonian $\omega_r a^\dagger a + \omega_q b^\dagger b - \frac{\chi_{qq}}{2}(b^\dagger b)^2$. We perform the first unconditional displacement D_β of the cavity

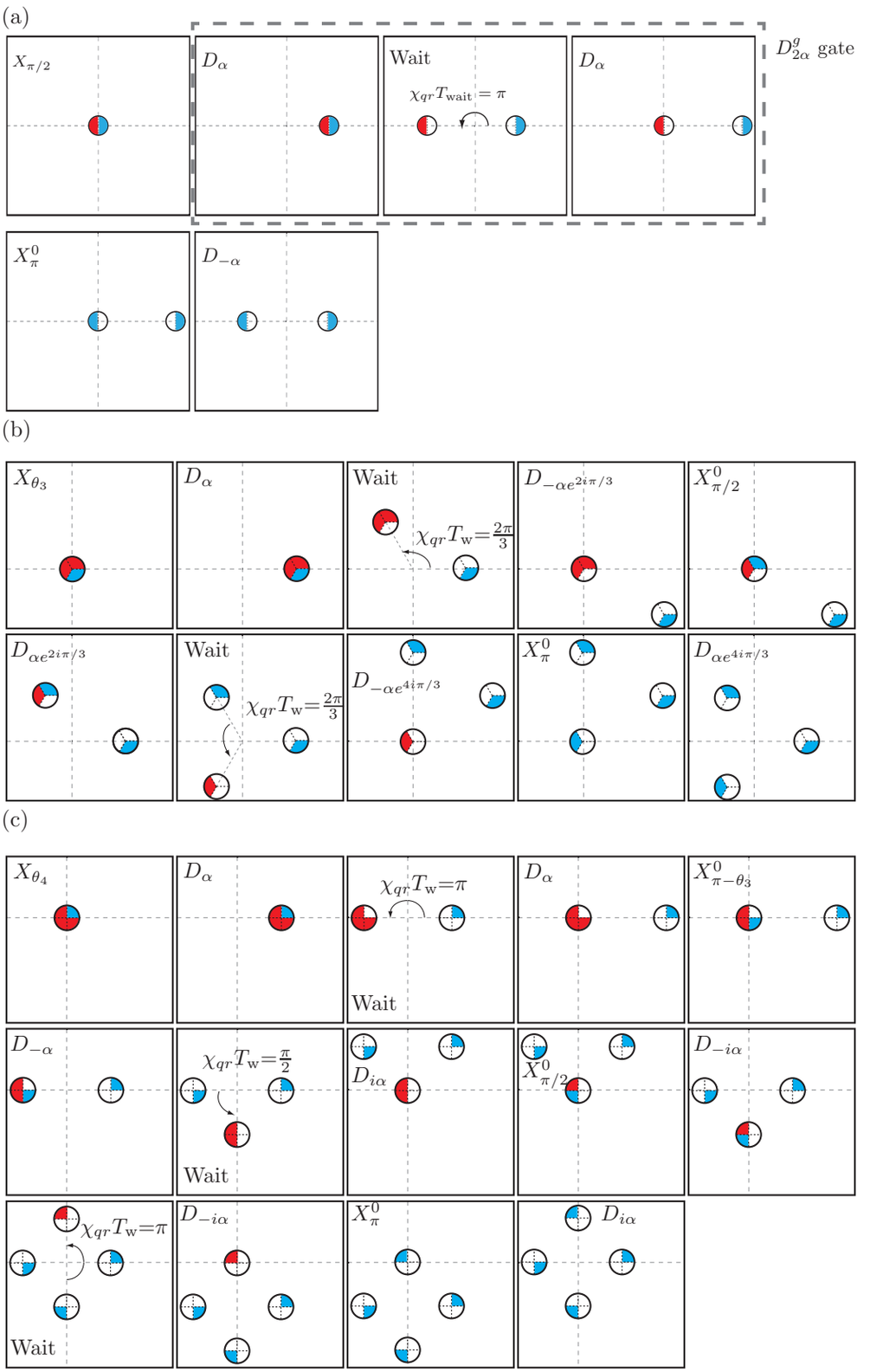

FIG. 5. (Color) Detailed sequence to prepare a superposition of two (a), three (b), and four (c) quasiorthogonal coherent states. Each frame is the Fresnel diagram of the field in the resonator. The two dotted lines represent two orthogonal quadratures and intersect at 0. The frames are ordered from left to right and top to bottom. A circle of center α in the diagram refers to a coherent state of amplitude α. The fraction of the circle colored in blue (red) corresponds to the population of the qubit which is in the ground state (excited state). For example, frame 3 in panel (a) corresponds to state $\frac{1}{\sqrt{2}}(|g,\alpha\rangle + |e,-\alpha\rangle)$. In particular we represent $\frac{1}{\sqrt{2}}|g,\alpha\rangle$ with the right circle ($+\alpha$), with a qubit in $|g\rangle$ (blue color) and a 50% population (half full). Fast (here considered instantaneous) displacements, D_γ, transform any coherent state $|\alpha\rangle$ to $|\alpha+\gamma\rangle$ regardless of the qubit state. The Fresnel diagram is in a rotating frame which leaves states of the form $|g,\alpha\rangle$ unchanged, while $|\psi(0)\rangle = |e,\alpha\rangle$ evolves as $|\psi(t)\rangle = |e,\alpha e^{i\chi_{\rm qr}t}\rangle$. The selective pulse X^0_θ rotates the qubit state when the resonator is in the zero photon state $|0\rangle$. Graphically, this corresponds to changing a fraction of the color of a circle centered at 0. In panels (b) and (c), $\theta_3 = 2\arccos(1/\sqrt{3})$, and in panel (c) $\theta_4 = 2\arccos(1/2)$. A symbol in each frame n gives the operation performed to go from frame $n-1$ to frame n.

through a very short pulse that displaces the cavity regardless of the qubit state. We wait for time $T_{\rm wait}$ and apply a second unconditional displacement, $D_{-\beta e^{i\chi_{\rm qr}T_{\rm wait}}}$. Neglecting the cavity self-Kerr, this sequence of operations leads to the following unitary evolution:

$$\begin{aligned}\mathcal{U} &= D_{-\beta e^{i\chi_{\rm qr}T_{\rm wait}}} e^{i\chi_{\rm qr}T_{\rm wait}a^\dagger a b^\dagger b} D_\beta \\ &= e^{-i|\beta|^2\sin(\chi_{\rm qr}T_{\rm wait})}|g\rangle\langle g| \otimes D_{\beta-\beta e^{i\chi_{\rm qr}T_{\rm wait}}} \\ &\quad + |e\rangle\langle e| \otimes e^{-i\chi_{\rm qr}T_{\rm wait}a^\dagger a}.\end{aligned}$$

Taking $\alpha = \beta - \beta e^{i\chi_{\rm qr}T_{\rm wait}}$, we have

$$\mathcal{U}|g,0\rangle = e^{-i|\beta|^2\sin(\chi_{\rm qr}T_{\rm wait})}|g,\alpha\rangle, \quad \mathcal{U}|e,0\rangle = |e,0\rangle.$$

Up to a phase term of $e^{-i|\beta|^2\sin(\chi_{\rm qr}T_{\rm wait})}$ that we can take into account in future qubit pulses, this is precisely the conditional displacement. In particular, as shown in [11], taking $T_{\rm wait} = \pi/\chi_{\rm qr}$, we have a conditional displacement of $\alpha = 2\beta$ in a time of $\pi/\chi_{\rm qr}$.

In Fig. 5, we provide the complete sequence of operations which generates superpositions of two, three, and four quasiorthogonal coherent components.

APPENDIX B: FIRST-ORDER EFFECT OF THE CAVITY SELF-KERR

Let us finish by a simple computation showing the first-order effects of the cavity self-Kerr. Considering a short time τ such that $\epsilon = \chi_{rr}\tau/2 \ll 1$, we can show that the first-order contribution of the cavity self-Kerr is simply an extra deterministic phase accumulation of the cavity's coherent states that we can take into account in future cavity displacements and qubit rotations. Indeed, the distortion of the coherent states happens only as a second-order term with respect to ϵ. Consider a coherent state, $|\alpha\rangle$, of average photon number $\bar{n} = |\alpha|^2$. We define $|\psi_\epsilon\rangle = e^{i\epsilon(a^\dagger a)^2}|\alpha\rangle$ and we search for a coherent state of amplitude α_ϵ and global phase ϕ_ϵ: $e^{i\phi_\epsilon}|\alpha_\epsilon\rangle$, which is close to $|\psi_\epsilon\rangle$ for small ϵ. We have $\langle\psi_\epsilon|a|\psi_\epsilon\rangle = \alpha e^{i\epsilon}e^{\bar{n}(e^{2i\epsilon}-1)} = \langle\alpha_\epsilon|a|\alpha_\epsilon\rangle$ for $\alpha_\epsilon = \alpha e^{i\epsilon}e^{\bar{n}(e^{2i\epsilon}-1)} = \alpha e^{i\epsilon(2\bar{n}+1)} + O(\epsilon^2)$. In order to find ϕ_ϵ, we compute

$$e^{-i\phi_\epsilon}\langle\alpha_\epsilon|\psi_\epsilon\rangle = e^{-i\phi_\epsilon}\langle\alpha|e^{i\epsilon(-(2\bar{n}+1)a^\dagger a+(a^\dagger a)^2)}|\alpha\rangle + O(\epsilon^2)$$
$$= e^{-i\phi_\epsilon}(1 - i\epsilon\bar{n}^2) + O(\epsilon^2).$$

Taking $\phi_\epsilon = -\epsilon\bar{n}^2$, we get $e^{-i\phi_\epsilon}\langle\alpha_\epsilon|\psi_\epsilon\rangle = 1 + O(\epsilon^2)$. Therefore, as a first-order approximation for the effect of the cavity self-Kerr, we have

$$e^{i\chi_{rr}\tau(a^\dagger a)^2/2}|\alpha\rangle \sim e^{-i\chi_{rr}\tau\bar{n}^2/2}\left|e^{i\chi_{rr}\tau(\bar{n}+\frac{1}{2})}\alpha\right\rangle.$$

In the simulations of this article, we took into account this extra coherent state rotation for the following displacements. The overall phases were corrected by adequately choosing the subsequent qubit pulse phases.

[1] A. Wallraff, D. I. Schuster, A. Blais, L. Frunzio, J. Majer, M. H. Devoret, S. M. Girvin, and R. J. Schoelkopf, Phys. Rev. Lett. **95**, 060501 (2005).

[2] J. Majer, J. Chow, J. Gambetta, J. Koch, B. Johnson, J. Schreier, L. Frunzio, D. Schuster, A. Houck, A. Wallraff *et al.*, Nature (London) **449**, 443 (2007).

[3] H. Paik, D. Schuster, L. Bishop, G. Kirchmair, G. Catelani, A. Sears, B. Johnson, M. Reagor, L. Frunzio, L. Glazman *et al.*, Phys. Rev. Lett. **107**, 240501 (2011).

[4] D. Gottesman, A. Kitaev, and J. Preskill, Phys. Rev. A **64**, 012310 (2001).

[5] M. Mariantoni, H. Wang, T. Yamamoto, M. Neeley, R. Bialczak, Y. Chen, M. Lenander, A. O. E. Lucero, D. Sank, M. Weides *et al.*, Science **334**, 61 (2011).

[6] X. Maître, E. Hagley, G. Nogues, C. Wunderlich, P. Goy, M. Brune, J. M. Raimond, and S. Haroche, Phys. Rev. Lett. **79**, 769 (1997).

[7] A. Megrant, C. Neill, R. Barends, B. Chiaro, Y. Chen, L. Feigl, J. Kelly, E. Lucero, M. Mariantoni, P. O'Malley *et al.*, Appl. Phys. Lett. **100**, 113510 (2012).

[8] M. Reagor, H. Paik, G. Catelani, L. Sun, C. Axline, E. Holland, I. Pop, N. Masluk, T. Brecht, L. Frunzio *et al.*, arXiv:1302.4408.

[9] W. Zurek, Nature (London) **412**, 712 (2001).

[10] J.M. Raimond, C. Sayrin, S. Gleyzes, I. Dotsenko, M. Brune, S. Haroche, P. Facchi, and S. Pascazio, Phys. Rev. Lett. **105**, 213601 (2010).

[11] C. M. Caves and A. Shaji, Opt. Commun. **283**, 695 (2010).

[12] M. Hofheinz, E. Weig, M. Ansmann, R. Bialczak, E. Lucero, M. Neeley, A. O'Connell, H. Wang, J. Martinis, and A. Cleland, Nature (London) **454**, 310 (2008).

[13] M. Brune, E. Hagley, J. Dreyer, X. Maître, A. Maali, C. Wunderlich, J. M. Raimond, and S. Haroche, Phys. Rev. Lett. **77**, 4887 (1996).

[14] S. Deléglise, I. Dotsenko, C. Sayrin, J. Bernu, M. Brune, J. M. Raimond, and S. Haroche, Nature (London) **455**, 510 (2008).

[15] Z. Leghtas, G. Kirchmair, B. Vlastakis, R. Schoelkopf, M. Devoret, and M. Mirrahimi, arXiv:1207.0679.

[16] D. Schuster, A. Houck, J. Schreier, A. Wallraff, J. Gambetta, A. Blais, L. Frunzio, J. Majer, B. Johnson, M. Devoret *et al.*, Nature (London) **445**, 515 (2007).

[17] L. Davidovich, A. Maali, M. Brune, J. M. Raimond, and S. Haroche, Phys. Rev. Lett. **71**, 2360 (1993).

[18] M. Silva and C. R. Myers, Phys. Rev. A **78**, 062314 (2008).

[19] B. Johnson, M. Reed, A. Houck, D. Schuster, L. S. Bishop, E. Ginossar, J. Gambetta, L. DiCarlo, L. Frunzio, S. Girvin *et al.*, Nat. Phys. **6**, 663 (2010).

[20] J. Koch, T. M. Yu, J. Gambetta, A. A. Houck, D. I. Schuster, J. Majer, A. Blais, M. H. Devoret, S. M. Girvin, and R. J. Schoelkopf, Phys. Rev. A **76**, 042319 (2007).

[21] S. E. Nigg, H. Paik, B. Vlastakis, G. Kirchmair, S. Shankar, L. Frunzio, M. H. Devoret, R. J. Schoelkopf, and S. M. Girvin, Phys. Rev. Lett. **108**, 240502 (2012).

[22] S. Haroche and J. M. Raimond, *Exploring the Quantum: Atoms, Cavities and Photons* (Oxford University Press, London, 2006).

[23] B. Yurke and D. Stoler, Phys. Rev. Lett. **57**, 13 (1986).

[24] L. G. Lutterbach and L. Davidovich, Phys. Rev. A **61**, 023813 (2000).

[25] C. Rigetti, S. Poletto, J. Gambetta, B. Plourde, J. Chow, A. Corcoles, J. Smolin, S. Merkel, J. Rozen, G. Keefe *et al.*, Phys. Rev. B **86**, 100506(R) (2012).

[26] G. Kirchmair, B. Vlastakis, Z. Leghtas, S. E. Nigg, H. Paik, E. Ginossar, M. Mirrahimi, L. Frunzio, S. M. Girvin, and R. J. Schoelkopf, Nature **495**, 205 (2013).

[27] K. Banaszek and K. Wodkiewicz, Phys. Rev. Lett. **82**, 2009 (1999).

[28] P. Milman, A. Auffeves, F. Yamaguchi, M. Brune, J. M. Raimond, and S. Haroche, Eur. Phys. J. D **32**, 233 (2005).

[29] A. Sarlette, Z. Leghtas, M. Brune, J. M. Raimond, and P. Rouchon, Phys. Rev. A **86**, 012114 (2012).

[30] D. Vitali, P. Tombesi, and G. J. Milburn, Phys. Rev. A **57**, 4930 (1998).

[31] S. Zippilli, D. Vitali, P. Tombesi, and J. M. Raimond, Phys. Rev. A **67**, 052101 (2003).

[32] S. Filipp, P. Maurer, P. Leek, M. Baur, R. Bianchetti, J. Fink, M. Göppl, L. Steffen, J. Gambetta, A. Blais *et al*., Phys. Rev. Lett. **102**, 200402 (2009).

[33] J. M. Chow, L. DiCarlo, J. M. Gambetta, A. Nunnenkamp, L. S. Bishop, L. Frunzio, M. H. Devoret, S. M. Girvin, and R. J. Schoelkopf, Phys. Rev. A **81**, 062325 (2010).

[34] T. Spiller, K. Nemoto, S. Braunstein, W. Munro, P. van Loock, and G. Milburn, New J. Phys. **8**, 30 (2006).

[35] K. Brown, Ph.D. thesis, University of Leeds, 2011.